THREE-DIMENSIONAL *A PRIORI* MODEL CONSTRAINTS AND UNCERTAINTIES FOR IMPROVING SEISMIC LOCATION

Megan P. Flanagan, Stephen C. Myers, Craig A. Schultz, Michael E. Pasyanos, and Joydeep Bhattacharyya

Lawrence Livermore National Laboratory

ABSTRACT

Accurate seismic event location is key to monitoring the Comprehensive Nuclear-Test-Ban Treaty (CTBT) and is largely dependent on our understanding of the crust and mantle velocity structure. This is particularly challenging in aseismic regions, devoid of calibration data, which leads us to rely on *a priori* constraints on the velocities. We investigate our ability to improve seismic event location in the Middle East, North Africa, and the Former Soviet Union (ME/NA/FSU) by using *a priori* three-dimensional (3-D) velocity models in lieu of more commonly used one-dimensional (1-D) models. Event locations based on 1-D models are often biased, as they do not account for significant travel-time variations that result from heterogeneous crust and mantle; it follows that 3-D velocity models have the potential to reduce this bias. Here, we develop a composite 3-D model for the ME/NA/FSU regions. This fully 3-D model is an amalgamation of studies ranging from seismic reflection to geophysical analogy. Our *a priori* model specifies geographic boundaries and velocity structures based on geology, tectonics, and seismicity and information taken from published literature, namely a global sediment thickness map of 1° resolution (Laske and Masters, 1997), a regionalized crustal model based on geology and tectonics (Sweeney and Walter, 1998; Bhattacharyya et al., 2000; Walter et al., 2000), and regionalized upper mantle (RUM) models developed from teleseismic travel times (Gudmundsson and Sambridge, 1998). The components of this model were chosen for the complementary structures they provide. The 1° sediment map and regionalized crustal model provide detailed structures and boundaries not available in the more coarse 5° models used for global-scale studies. The RUM models offer improved resolution over global tomography, most notably above depths of 300 km where heterogeneity is greatest; however, we plan to test other published upper mantle models of both *P*- and *S*-wave velocity.

We compute travel times through this integrated model for comparison with other standard 1-D models, as our goal is to evaluate whether the 3-D model can better predict the observed travel times. The arrival times are computed through the model using a 3-D finite-difference technique and are then compared with a declustered set of ISC *P* arrival times (Engdahl et al., 1998). Our ME/NA/FSU model predicts the *P* and *Pn* travel times very well, as measured by variance reduction, for three stations we tested: ARU, KVT, and GAR; these predicted times also resemble some patterns seen in *Pn* tomography models of this region. Such tests will allow us to identify parts of the model that may need modification.

We also compute model-based correction surfaces for each station in the ME/NA/FSU regions that can be used as additional constraints in our event location algorithm to determine the improvement provided by using 3-D models. We use this method to relocate a set of ground truth events: the 1991 Racha aftershock sequence which was investigated by Myers and Schultz (2000) using empirical kriged correction surfaces and a 1-D velocity model. They find an epicenter mislocation bias of 42 km when no corrections are applied and that this mislocation is reduced to 13 km when their empirically derived correction surfaces are included. We relocate this same set of events using our model-based correction surfaces and produce a mislocation bias of only 26 km, a significant improvement. We are currently implementing methods to quantify uncertainties on the model-based corrections which will be required to compute representative error ellipses for the new locations. We also plan to combine both the model-based and empirical correction techniques to achieve the best improvement in location. This test case demonstrates the power of using 3-D velocity models to improve location capability for small, regionally recorded events. This example also shows how the model-based approach holds great potential for improving locations in aseismic regions where it may not be possible to compute empirical correction surfaces.

Key Words: travel time corrections, model-based correction surfaces, 3-D velocity model, event location

OBJECTIVE

High quality regional velocity models are necessary for accurate seismic locations required for monitoring the Comprehensive Nuclear-Test-Ban Treaty (CTBT). A common approach to seismic location has been to use a one-dimensional (1-D) velocity model and apply source-specific station corrections to remove bias due to three-dimensional (3-D) Earth structure. Such corrections yield more accurate travel-time predictions and hence more accurate location of the seismic event; however, they do not provide source-specific uncertainties for the new locations.

Empirical kriged corrections and other model optimization methods are well suited to improve travel-time prediction in areas where ground truth (GT) events are available; however, vast portions of the ME/NA/FSU are devoid of GT events (*e.g.*, North Africa, Russia). In order to improve travel-time prediction at regional and near teleseismic distances in regions without GT calibration, we have developed the *a priori* 3-D velocity model MENAFSU1.0. We seek to validate our *a priori* 3-D velocity model MENAFSU1.0 and use this model to locate a regionally recorded set of GT events. The new locations are compared to those computed using a 1-D velocity model and empirically derived kriged correction surfaces, and the improvement in location using our model-based correction surfaces is demonstrated in an end-to-end case study.

RESEARCH ACCOMPLISHED

Middle East, North Africa, and Former Soviet Union 3-D velocity model (MENAFSU1.0)
This regionalized model is a preliminary set of geophysically distinct regions that can be used for estimating travel-times, surface wave dispersion, and discrimination properties particularly in aseismic regions where calibration data is sparse. The model can also provide a platform for assessing progress in seismic location, discrimination, detection—the entire calibration process—and aid in determining the priority and planning of calibration
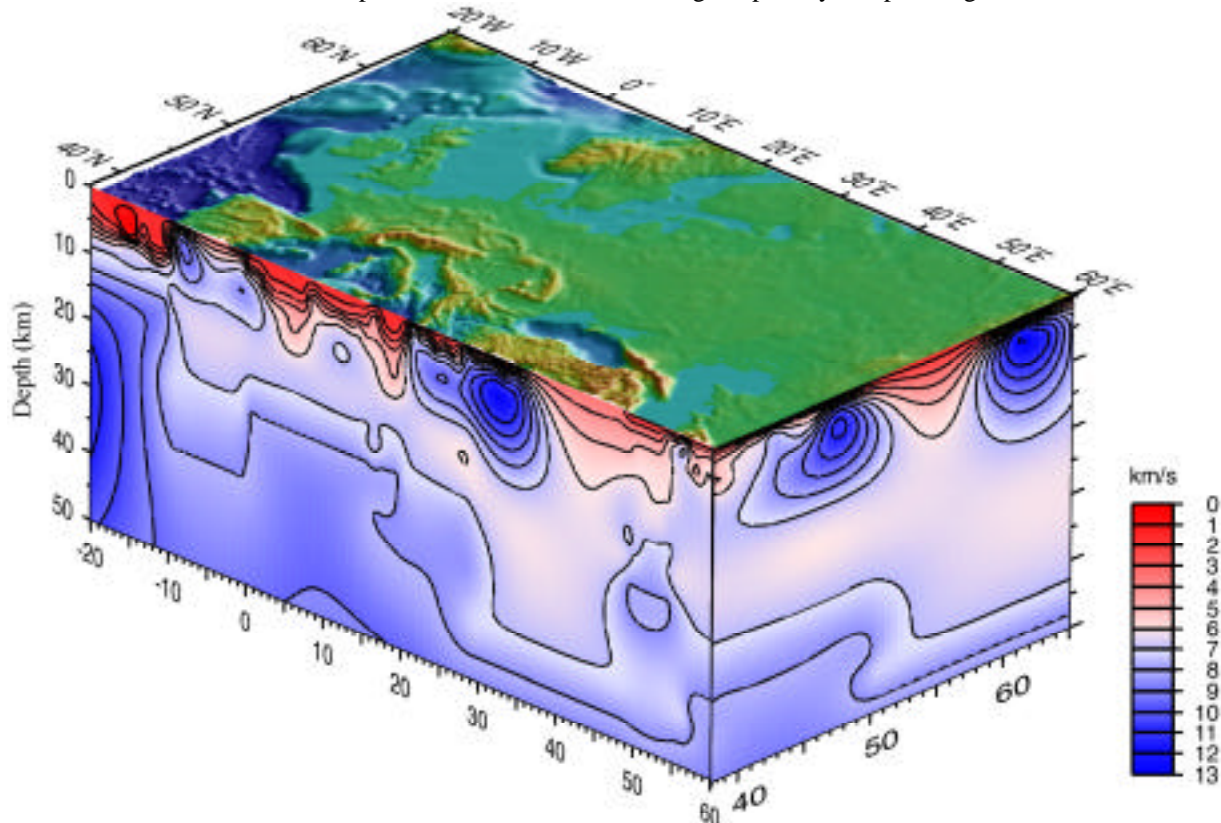

Figure 1. Cross-section of *P*-wave velocities from our 3-dimensional MENAFSU1.0 model.

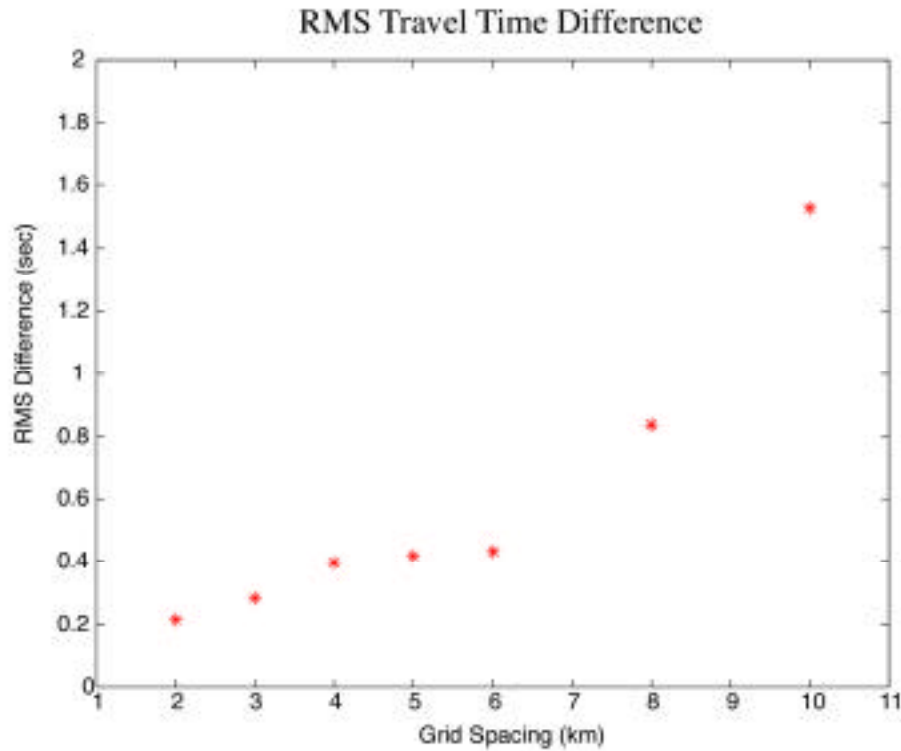## RMS Travel Time Difference

Figure 2a. The RMS travel time difference is reduced when a smaller grid spacing is used in the 3-D finite difference computation; this RMS error is the difference between travel time calculated through the FD code and that calculated using a 1-D ray-tracer (CalcTT) through the *AK135* velocity model.
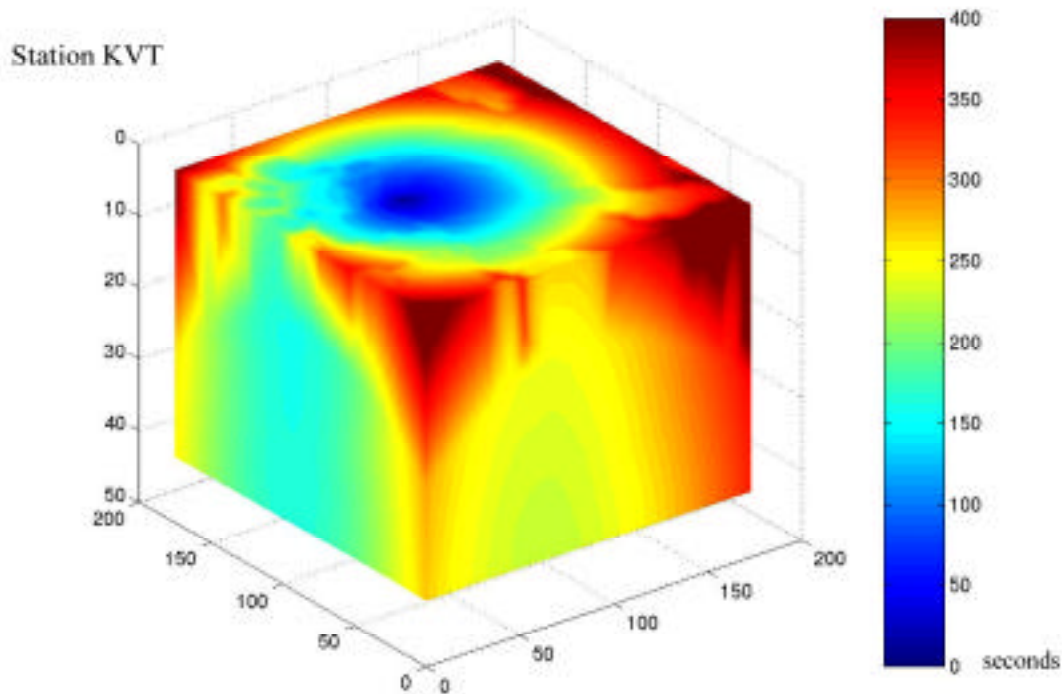

Figure 2b. This volume of travel times is the output from the 3-D finite difference calculation. The 3-D velocity structure causes the travel times to be asymmetric about the station KVT, which is located at zero time (bright blue spot in center). Arrival times for *P* and *Pn* phases for specific source-station paths are extracted from this volume by interpolation. Note the axes are units of 10 km, and the colors are time in seconds.

experiments. Our goal is to build a reference model for the region that can be used in making model-based correction surfaces. This model has been used to derive predictions of surface wave dispersion curves and regional travel times for comparison with data. In addition, empirical observations are being used to further refine the background geophysical model. The MENAFSU1.0 model specifies geographic boundaries and velocity structures based on geology, tectonics, and seismicity. This regionalization serves as a starting point, and we expect to refine and improve upon it based on such tests as predicting P and Pn travel times (presented here) as well as surface wave velocities. As the model improves and demonstrates some predictive power, it may evolve into a base model for tomographic inversions as well as a reference model for other CTBT-related research efforts.

The entire area is divided into 31 regions selected primarily on the basis of seismicity patterns, tectonic history, crustal thickness, and crustal velocity (Bhattacharyya et al., 2000; Walter et al., 2000). Each region is composed of 7 homogeneous layers for water, unconsolidated and consolidated sediments, upper crust, middle crust, lower crust, and upper mantle half-space, following the specifications of Mooney et al. (1998) in their 5° resolution model *CRUST5.1*. We have stripped off and replaced the sediments with a high-resolution 1° sediment model (Laske and Master*s*, 1997) and have discretized all 31 regions into 1° latitude and longitude blocks while the depth layers remain variable in thickness. A representative cross-section of the velocity model is shown in Figure 1. We have added a regionalized upper mantle model below the *Pn, Sn* velocity layers. Of the many upper mantle models available, we have chosen initially to use the *RUM* (Regionalized Upper Mantle) model of Gudmundsson and Sambridg*e* (1998). This model is attractive for two reasons; first it follows a similar regionalization procedure as was used for the crust except applied to the mantle. Second, it is based on deviations from *AK135* (Kennett et al., 1995) which is our basis for calculating travel times.

The MENAFSU1.0 velocity model is an amalgamation of geophysical and geological studies, constituting a self-consistent 3-dimensional Earth model for the crust and upper mantle. Because the MENAFSU model is 3-D, region-specific velocity structure, it can be characterized more accurately than 1- or 2-D models. While this model comprises *P*-wave, *S*-wave, density, and attenuation, we use only the *P*-wave structures at this time.

Finite Difference Travel-Time Calculations
We use an algorithm originally developed by Vidale (1988) and further refined by Hole and Zelt (1995) which uses a finite difference (FD) approximation to the Eikonal equation to compute first arrival travel times through regularly gridded velocity structures. This technique approximates Huygen's principle by propagating wavefronts radially outward from a point source using each grid (or time) node as a secondary source for each successive grid node. This procedure is more efficient and accurate than ray tracing as it is able to account for sharp velocity gradients which can produce different propagation modes (*e.g.*, refracted and diffracted body waves, head waves) in addition to direct phases. Furthermore, because the travel times are computed for every grid point in the volume, the code is much faster than tracing rays from a single event to a large number of receivers. In fact, we use the principle of reciprocity by placing the source point at the seismic station location and interpolate the travel times computed at each grid node to match the exact earthquake location (Flanagan et al., 1999).

We modify the original code in two ways. First, we adapt it to read in 3-D velocity models instead of 1-D such that it can compute times through our MENAFSU1.0 (or any custom 3-D) model. Second, we apply a Cartesian to spherical coordinate transformation to the source and receiver locations that are input to the code (K. Koper, personal communication, 1999). These modifications are necessary as we need to compute travel times out to regional and near-teleseismic distances (~13° to 30°) while the original FD algorithm operates in Cartesian coordinates, which are accurate only for distances of up to 300 km in the Earth. To account for the curvature of the Earth one option is to apply an Earth flattening transformation; however, this is only strictly valid for 1-D velocity models and not for our 3-D model. We develop the spherical coordinate transformation scheme in which we parameterize a spherical surface inside the Cartesian volume of grid nodes. Here, the source and receiver positions and velocity model are known in spherical coordinates, and they are transformed into the Cartesian system as input to the FD code. The finite difference operators remain unchanged, and the output is converted to spherical coordinates as well.

The FD algorithm requires our velocity model to be discretized on to an equally spaced grid; this requires fine sampling, by linear interpolation, of our 1° by 1° velocity model. This procedure results in the loss of some resolution with depth (*e.g.*, some sediment layers may be thinner than the grid size) and an oversampling of lateral structure as the velocities in the shallower part of the model vary more rapidly with depth than they do laterally.

Our fully 3-D code is run in a volume of dimensions of roughly 30° by 30° laterally and 800 to 1000 km deep with a grid spacing of 3 km; the exact latitude-longitude bounds of the volume vary with each station. The grid spacing is determined empirically as a trade-off between the accuracy of the travel-time prediction and computer memory limitations as both the velocity grid (or slowness) and the travel-time grid must be held in memory simultaneously. Our current resources limit us to grids with about 350 million nodes which requires approximately 4 Gbytes of computer memory. After a number of tests running the code with incrementally smaller grid sizes and comparing the resulting travel times with those computed using a simple 1-D ray tracer, we find that a grid spacing of 3 km provides a reasonable accuracy as shown in Figure 2a. Accuracy and errors of the FD code arise from grid boundary effects and from the discrete approximation of the differencing algorithm. These accuracies are being evaluated through convergence tests and through careful comparisons with known solutions; currently the RMS errors appear to be less than 0.5 seconds (Figure 2a). Absolute errors and accuracy are being derived in seismic areas where we can statistically assess the ability of this *a priori* model to predict data.

The outputs from the FD code are two 3-D volumes: one of the *P*-wave velocity at each grid node and one of the *P* arrival time at each node; an example of the travel-time volume is shown in Figure 2b as computed for station KVT. We perform two runs for each station of interest, once using the MENAFSU1.0 and once using the global reference model *AK135*; we then compare times from each of these volumes for the same source-station paths.

Validation of Travel-Time Improvement

To test the predictive power of the MENAFSU1.0 model, we compute the median residuals between the observed *P* and P_n arrivals at each station and the arrivals predicted by both our MENAFSU1.0 model and the *AK135*. We use *P* and P_n travel-time picks from a relocated subset of earthquakes in the ISC Bulletin (Engdahl et al., 1998) which have been further processed with a declustering algorithm. This entails filtering spatial data with the goal of consolidating heavily clustered points into small collections of representative data points with associated uncertainties. This technique is intended to reduce the extremely large set of arrival times into a smaller more manageable data set with minimal loss of information. As part of the process, outliers within data clusters are removed and the uncertainty estimates for the improved data set are provided.

Travel-time residuals are computed by interpolating between grid nodes to calculate the predicted arrival time for an exact source-station path. This is done for both the MENAFSU1.0 travel-time volume and the *AK135* travel-time volume, and each predicted time is subtracted from the observed arrival time. These residuals (observed - predicted time) for station ARU and KVT are shown in histogram form in Figure 3. The 3-D MENAFSU1.0 model predicts the observations very well, showing a significant variance reduction, while for others it does not improve the fit given by the *AK135*. This procedure will help us identify regions where the model needs to be improved
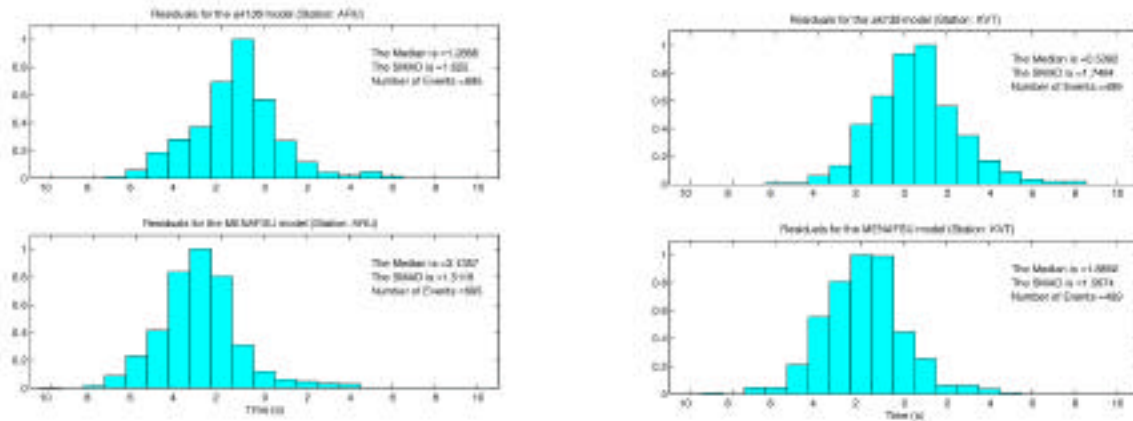

Figure 3. Travel-time validation for the MENAFSU1.0 model at example stations ARU and KVT. In general, travel-time variance for the MENAFSU1.0 model is reduced compared to the *AK135* model. In some instances the mean of the distribution is displaced from zero; however, this may be due to optimization of event origin times relative to the *AK135* model.

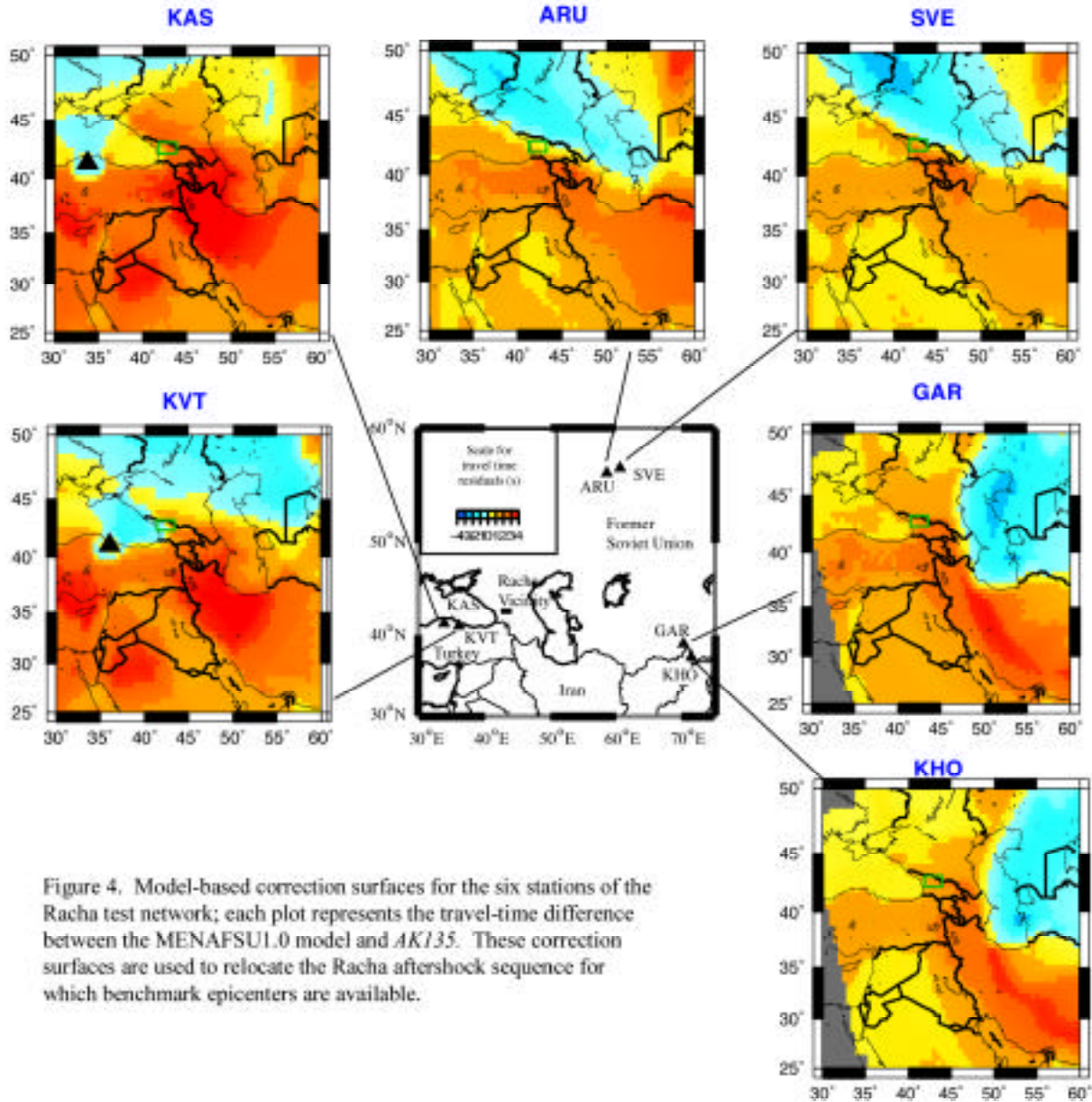## Model-Based Correction Surfaces

Figure 4. Model-based correction surfaces for the six stations of the Racha test network; each plot represents the travel-time difference between the MENAFSU1.0 model and *AK135*. These correction surfaces are used to relocate the Racha aftershock sequence for which benchmark epicenters are available.

Model-Based Correction Surfaces

To compute model-based correction surfaces we subtract the *AK135* predicted time from the MENAFSU predicted time along a regular grid in latitude, longitude and at a depth of 10 km. Examples of these surfaces are shown in Figure 4 for the six stations we will use in our relocation test described below. Each correction surface provides station-specific travel-time corrections for regional to near-teleseismic distances providing improved accuracy and precision for travel-time predictions. We find travel time differences of up to 6 sec relative to *AK135*, most in areas of very thick crust or sediment (blue indicates fast regions and red indicates slow). Note the patterns in these correction surfaces correlate with the structural features in the MENAFSU1.0 model; fast predictions are seen to the north on the Russian platform while slow anomalies are seen at the southern Caspian as well as eastern Turkey and the southern Caucasus.

Next we determine the improvement provided by the 3-D models by relocating a set of ground truth events. We use the model-based correction surfaces computed for six stations (KAS, KVT, GAR, KHO, ARU, and SVE)

comprising the test network which recorded the 1991 Racha aftershock sequence; these surfaces are plotted in Figure 4. The fast and slow residual patterns seen in these correction surfaces show strong similarities to the patterns seen in the empirical kriged correction surfaces based on 1-D velocity models Myers and Schultz (2000).

Improving Location: The 1991 Racha Aftershock Sequence

The improvement in seismic location that is gained by using our *a priori* 3-D velocity model is the ultimate test of this method's utility. We use a set of GT2 locations determined using regionally recorded aftershocks in the region of Racha, Georgia. These GT locations are then compared with our locations computed using our model-based correction surfaces, and we assess the degree to which our 3-D velocity model accounts for some of the differences that are indicated by the path corrections and spatial differences in arrival times to each of the six stations (Flanagan,et al., 2000).

In a previous study, Myers and Schultz (2000) demonstrated location improvement using Modified Bayesian Kriging (MBK) to compute empirical correction surfaces for the sparse 6-station test network. The MBK correction surfaces for the test-network stations are based on high-quality teleseismically constrained hypocenters throughout the Middle East (Engdahl et al., 1998). The 1991 Racha events are then relocated with and without the aid of MBK correction surfaces, and the resulting epicenters are compared to the benchmark GT2 locations determined from a dense local deployment of seismic sensors. When no travel-time correction is applied, the mean horizontal distance between the local and test network locations is 42 km, and there is a distinct bias in sparse-network locations towards the north-northwest. The mean difference between local and sparse network locations is reduced to 13 km when the empirical corrections are applied and the bias in location is significantly reduced (Figure 5, center).
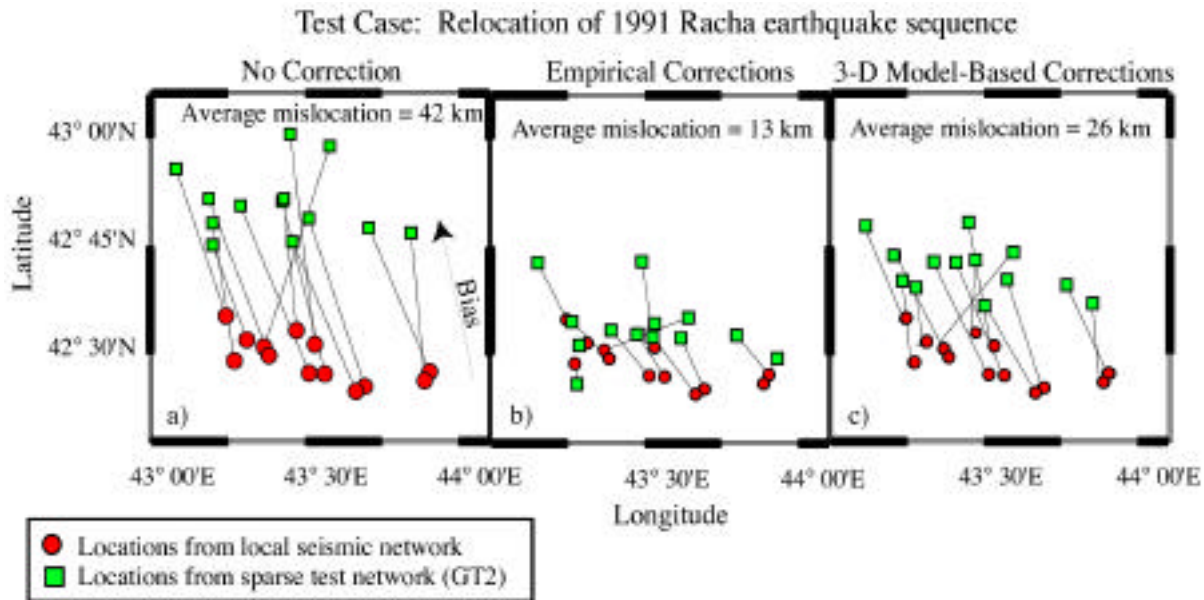

Figure 5. Location bias is significantly reduced when either empirically dervived or 3-D model-based corrections are applied to reduce travel-time prediction inaccuracies.

Next we relocate the Racha events with and without our new model-based correction surfaces (shown in Figure 4) as constraints, and the resulting epicenters are compared to benchmark GT2 locations. The mean difference between the benchmark and test network locations is reduced from 42 km to 26.6 km when the model-based corrections are applied, and the bias in location is significantly reduced (Figure 5, right). This reduction is almost as large as that achieved when the empirical kriged correction surfaces are applied. We are currently implementing methods to derive uncertainty estimates for the model-based correction surfaces which will be required to compute representative error ellipses for the new locations. Since our *a priori* MENAFSU1.0 model does not have

uncertainties associated with it, we must use the misfit between the observed travel times and those predicted from our model as a measure of uncertainty (see Figure 3).

This test case demonstrates the power of 3-D model-based corrections to improve location of small, regionally recorded events. This model-based approach shows enormous potential for improving location in aseismic regions, where GT events are not available. However, this relocation of the Racha sequence should be viewed with caution as we continue to test and evaluate the predictive power of the MENAFSU1.0 velocity model in other regions.

CONCLUSIONS AND RECOMMENDATIONS

Empirically derived correction surfaces are applicable where GT events exist, but extrapolation of travel-time corrections from GT events is quickly damped to the background statistics of the *AK135* model in regions where there are no data to constrain the corrections. Therefore, model-based corrections, which are shown here, are better suited to improve travel-time prediction and thus location capability in areas devoid of GT events.
The test case relocation of the 1991 Racha sequence should be viewed as a one-point validation of our 3-D model. Additional validation of the predictive power of the MENAFSU1.0 velocities is being actively pursued in other high-quality GT regions. Further testing of the FD code for grid size *vs.* accuracy of the predicted travel time is underway as we investigate variable grid spacing techniques to allow us to compute times for smaller grid spacing and geographic areas larger than 30°. We are also compiling a large data set of shear wave arrival times to test and validate the *S*-wave velocity structure of MENAFSU1.0 as our FD code can easily compute first arrival times for shear waves.

REFERENCES

Bhattacharyya, J., W. Walter, M. Flanagan, J. O'Boyle and M. Pasyanos, (2000) , Preliminary Definition of Geophysical Regions in Western Eurasia, UCRL-ID-138402.

Engdahl, E.R., R. van der Hilst, and R. Buland, (1988) Global Teleseismic Earthquake Relocation with Improved Travel Times and Procedures for Depth Determination, *Bull. Seismol.. Soc. Am., 88*, 722-743.

Flanagan, M. P., C. A. Schultz, and L. J. Hutchings, (1999) Development of 3-D Crust and Upper Mantle Velocity Models to Improve Seismic Event Location, AGU Fall Meeting, San Francisco, CA, *EOS Trans. Am. Geophys. Un., 80,* p. F656.

Flanagan, M. P., S. C. Myers, M. E. Pasyanos, C. A. Schultz, W. R. Walter, K. D. Koper, (2000) Improving Regional Event Locations in the Middle East by Incorporating Model Based Correction Surfaces Derived from 3-D Velocity Structures, SSA Spring Meeting, San Diego, CA, *Seismol. Res. Lett., 71,* p. 184.

Gudmundsson, O., and M. Sambridge, A Regionalized Upper Mantle (RUM) Seismic Model, (1998) *J. Geophys. Res., 103*, 7121-7136.

Hole, J.A. and B.C. Zelt, 3-D Finite Difference Reflection Travel Times, (1995) *Geophys. J. Int., 121*, 427-434.

Kennett, B.J.N., E.R. Engdahl and R. Buland, (1995) Constraints on Seismic Velocities in the Earth from Travel Times, *Geophys. J. Int, 122*, 108-124.

Laske, G. and T.G. Masters, (1997) A Global Digital Map of Sediment Thickness, *EOS Trans. AGU, 78*, F483.

Mooney, W. D., G. Laske, and T. G. Masters, (1998) CRUST 5.1: A global crustal model at 5° X 5°, *J. of Geophys. Res., 103*, 727-747.

Myers, S.C., and Schultz, C.A., (2000) Improving Sparse Network Seismic Location with Bayesian Kriging and Teleseismically Constrained Calibration Events, *Bull. Seismol. Soc. Am., 90*, 199-211.

Sweeney, J. and W. R. Walter, (1998) Preliminary Definition of Geophysical Regions for the Middle East and North Africa, UCRL-ID-132899.

Vidale, J., (1988) Finite-difference Calculation of Travel Times, *Bull. Seismol. Soc. Am., 78*, 2062-2076.

Walter, W.R., M.E. Pasyanos, J. Bhattacharyya and J. O'Boyle, (2000) MENA 1.1 – An Updated Geophysical Regionalization of the Middle East and North Africa, UCRL-ID-138079.